

Iteratively re-weighted least squares inversion for the estimation of density from well logs: part one

A. Nassir Saeed, Laurence R. Lines, and Gary F. Margrave

ABSTRACT

A quantitative analysis of density log is established in this study by inverting of density log. The re-weighted inverse algorithm of density log using different constraints in model-structure space have shown stable and fast convergence towards the final model with few numbers of iterations. The inverted density model has resolved different lithology layers, and successfully delineated gas-bearing sand reservoir of the Blackfoot.

INTRODUCTION

A common practice in the oil & gas industry is to follow qualitative approach by plotting density logs without estimating uncertainty, and correlate them to other logs. For clastic rocks, petrophysicists and geophysicists normally use the empirical Gardner equation (Gardner et al., 1974) below to approximate density (ρ) from P-wave (V_p).

$$\rho = aV_p^q \quad (1)$$

where $a=0.31$, $q=0.25$ and V_p in m/sec

This classical approach, often neglects drilling condition and other circumstances that affect specific well bore log during the course of survey. Others mistakenly apply equation (1) to carbonate rock that would generate erroneous density data, thus producing incorrect acoustic impedance for this type of rock. Thus, a need for developing new technique so as to estimate the uncertainty in density log has become imminent. Therefore, the main objective of this study is to quantify the density log via the Inverse theory, and to produce more interpretive section of inverting density log.

GEOLOGY OF STUDY AREA

The Blackfoot field represents a common style of stratigraphic trap in the Western Canadian Basin (Pendrel et. al, 1999). The field is located near Strathmore in south central Alberta, approximately 100 km east of Calgary. The producing formation is cemented channel sand (Glaucinitic of the Lower Cretaceous age) deposited as incised valley-fill sediments above the Mississippian carbonates (Wood and Hopkins 1992). Well log 08-08, which located in the produced formation, is used in this study (figure 1).

The Glaucinitic-incised valley complex consists of three different components: Upper, Lithic, and Lower. Only the Upper and Lower valleys are prospective in this area (Dufour et al., 1998), while Lithic is non-porous barrier between upper and lower valleys. The Glaucinitic sandstone is up to 35m thick and is approximately 1550m below the surface in the Blackfoot area (Margrave et. al., 1998).

Differentiation of prospective porous sandstone and non-productive shale poses a problem due to the similarity in their stacked impedances (Miller et al., 1995). Research studies that are conducted in this area (Goodway and Tessman, 2002; Chopra and Pruden, 2003) suggested to the use of V_p/V_s as a DHI in discriminating between productive sandstone and barrier shale.

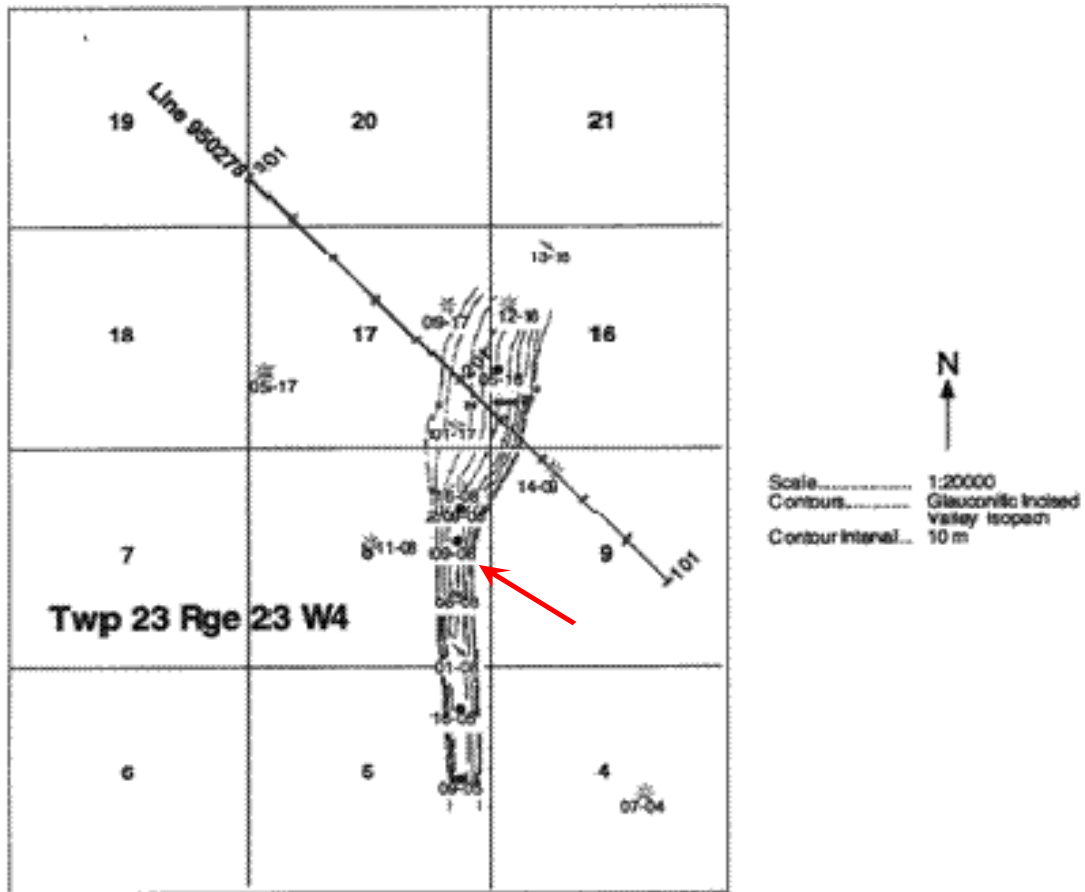


FIG.1. Location map of 3C-2D Seismic line, well control and incised Valley Isopach (after Miller et. al. 1995). The red arrow points to the location of Well 08-08.

The sonic V_p , V_s , V_p/V_s and density logs of Well 08-08 are showing in figure (2). Note that the density log does not show a distinct change at the top boundary of Mississippian formation compared to the V_p and V_p/V_s log graphs from that well.

The density log in figure (2) raises the following questions:

- 1) How accurate/reliable is the density log?
- 2) Is it possible to discriminate between prospective sandstone and non-productive shale? Can we separate between detriatal and Mississippian carbonate regions using density log only?
- 3) Can we conduct quantitative analysis for density log rather using conventional qualitative approach?

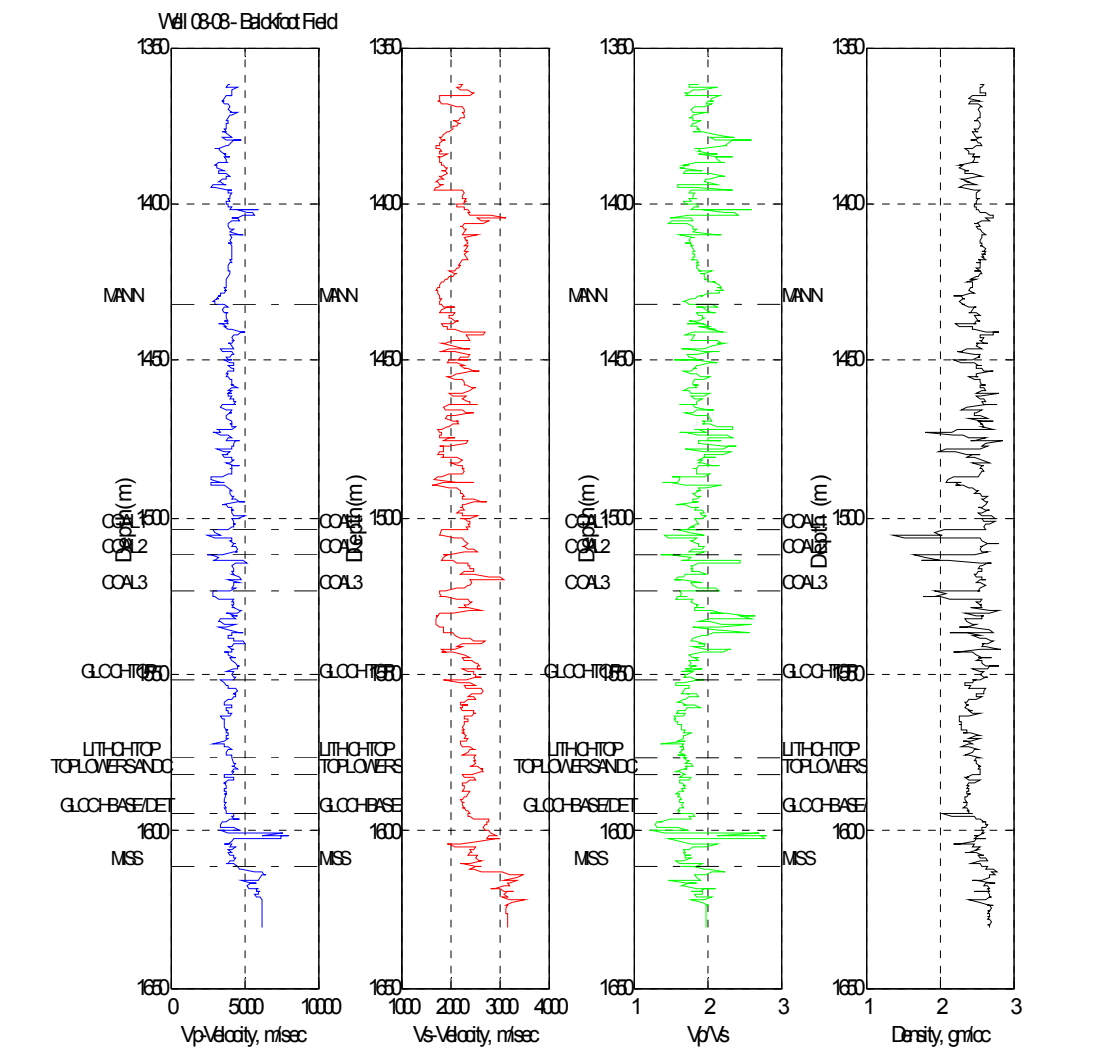


FIG. 2. Well 08-08: P-wave (V_p), S-wave (V_s), V_p/V_s and density (RHOB) logs

INVERSE PROBLEM

In order to answer questions mentioned in previous section, we need to re-calculate field data, trying to fit the synthetic model to measured data and then estimating data misfit or uncertainty. Producing a model that describes our observed data to a certain degree of confidence is the core subject of the inverse theory (Tarantola, 1987). Density log can be posed as an inverse problem and solved accordingly. By taking the logarithm of Gardner equation yields

$$\ln(\rho) = \ln(a) + q * \ln(Vp) \quad (1a)$$

The forward – inverse density pair can be written as:

$$m = G^T d \quad (2)$$

$$d = Gm + \varepsilon \quad (3)$$

The general approach is to use the linear regression method of best fit line, where Gardner constants can be derived locally. In this method, we estimate the slope and exponent of intercept point of best-fit line through semi-log scale of Vp scatter graph (Figure 3), and then substitute them for a and q in equation (1) in order to calculate the predict density. Thus, better approximations of borehole conditions are included.

Figure (4) shows the observed-, default Gardner- and locally derived- density logs plotted along with the P-wave (Vp) log. Note the change in derived density log shape at depth 1600m where Mississippian formation manifests. The spike-like shape in predicted density log prompts us to research for an inverse method so as to investigate the problem further in order to confirm if the spike change in density log at specific depth level is merely due to outliers or lithology change.

In Least-squares inversion, we solve for a parameter model vector, m , which fits a model response, f , to data, d , in a least squares sense (Lines and Treitel, 1984). The error in equation (3) is assumed to be white noise (Aster et. al., 2005). Traditional Tikhonov regularization selects solutions by minimizing an objective function (equation 4) that combine the ℓ_2 norm of data-misfit and semi-norm of model length (equation 5).

$$\phi = \phi_d + \lambda \phi_m \quad (4)$$

$$\phi(m) = \|Gm - d\|_2^2 + \lambda^2 \|Gm\|_2^2 \quad (5)$$

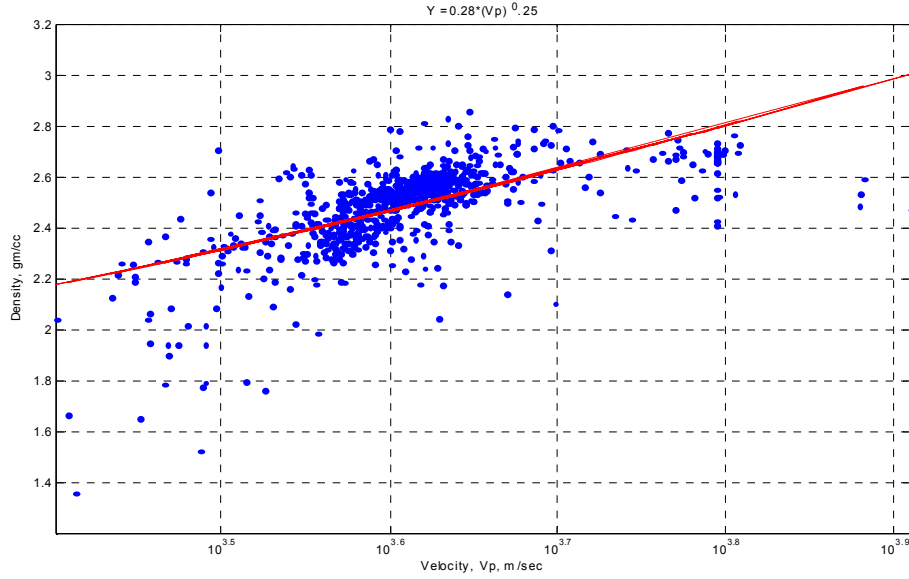


FIG.3. Well 08-08: Semi-log velocity versus density for estimating a and q via linear regression method. Values of a and q were 0.25 and 0.28 respectively.

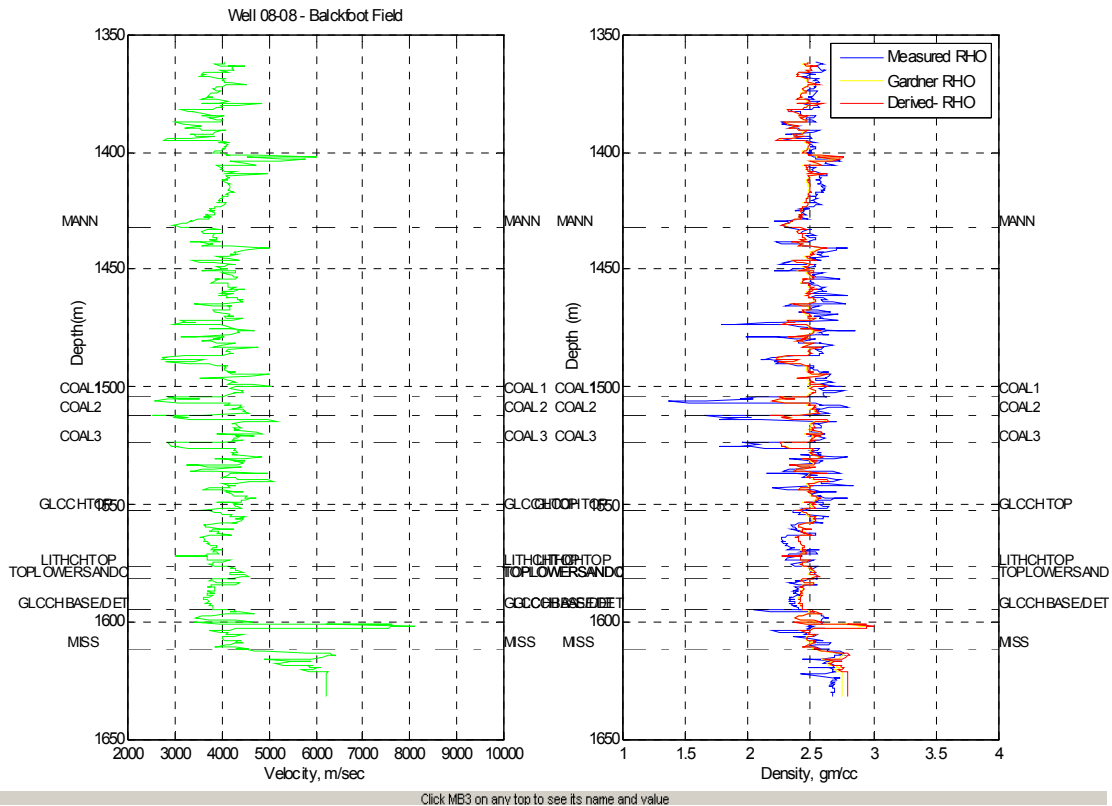


FIG.4. Well 08-08: Measured-, default Gardner, and locally derived – density logs along with sonic Vp log.

The Levenberg-Marquardt least squares inverse equation (Levenberg, 1963) can be written as

$$(G^T G + \mu_i I)m = G^T d \quad (6)$$

where G is the forward operator, I is identity matrix and is μ regularization parameter.

The regularization parameter or damping factor, μ , is the trade-off parameter between the residual norm and model norm. If μ is a relatively large number, the noise will be attenuated at the expense of a less accurate approximation of the desired output, thus it degrades the resolution of the density log. On the other hand, If μ is too small, the noise could dominate the output density log, which leads to instabilities in the inversion. Therefore, addition of a damping factor is a trade off between accuracy and instabilities in the inverse algorithm.

There are many approaches for selecting a proper value of regularization parameter. The L-curve method (Hansen and O'Leary, 19993) is based on a maximum curvature. On the other hand, the discrepancy principle or generalized cross-validation method, GCV, (Wahba, 1977) is another used approach. Both techniques require solving equation (6) for different range of damping factor; a potentially very costly task.

In this study, a damping factor of 0.1 is used in the initial iteration. For subsequent iterations, the damping factor is either increased by 0.25 of μ_{i-1} or decreased by magnitude of $\mu_{i-1} / 4$. This is because computed damping factors have produced stable and good convergence for inverted model. Increasing or decreasing of regularization parameter is bound by the magnitude of ℓ_2 norm of the model length for ϕ_m^i and ϕ_m^{i-1} . For the 1st iteration, I chose the norm of logarithmic measured data as an initial norm condition of model length. Figure (5) shows the Lagrange multiplier, μ_i for i^{th} iterations during inversion of density log.

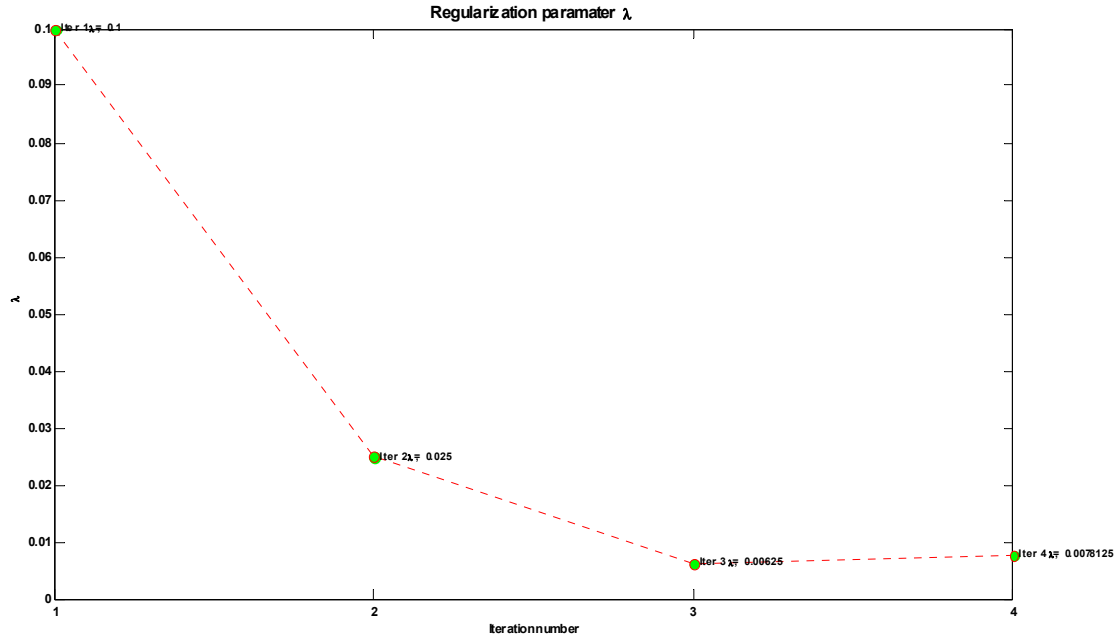


FIG.5. Well 08-08: IRLS inversion. The Lagrange multiplier, μ_i for i th iterations during inversion of density log.

IRLS INVERSION OF DENSITY LOG

In this study, the Lagrange Inverse equation, which is a modified version of equation (6) is used. The Lagrange equation is widely used and proved to be stable when redundant data points are collocated at same location. This in fact, suites field data acquisition of density logging where density equipment are lowered to a certain depth level, and several measurements are collected over a constant time before moving logging equipments to next depth level.

We formulate the inverse problem using Tikhonov regularization (Tikhonov and Arsenin, 1977) to obtain inverse solution by minimizing objective function in equation (4).

The data misfit is defined as,

$$\phi_d = \|W_d(Gm - d)\|_2^2 \quad (7)$$

While the model solution is defined as,

$$\phi_m = \|W_m(m)\|_2^2 \quad (8)$$

A new objective function that incorporate different weights is then expressed as

$$\phi(m) = \|W_d(Gm - d)\|_2^2 + \lambda \|W_m(m)\|_2^2 \quad (9)$$

Thus, a new system of equation that provide an estimate of unknown parameter can be written as,

$$(G^T W_d^T R_d W_d G + \lambda W_m^T R_m W_m)m = G^T W_d^T R_d W_d d \quad (10)$$

where R_d and R_m are data misfit and model-structure weighting matrices (Farquharson and Oldenburg, 1998) introduced so that different elements of the data misfit and model roughness vectors are given equal weights in the inversion process. W_d is diagonal weighted matrix in the data space, while W_m is weighted or roughness operator in the model space.

In the following subsections, several types of weights (constrains) used in the data-misfit and regularization model norms are explained in some details.

Minimization using ℓ_1 measures of R_d and R_m

The general form of an objective function to be minimized (Scales et al., 1988) can be written as,

$$\phi(x) = \sum_j |x_j|^p \quad (11)$$

Traditional least square problem that satisfy ℓ_2 solved for $p=2$. If ℓ_1 is sought, then $p=1$, and the objective function is merely sum of absolute value of vector x . The vector x represents either data-misfit term (equation 12) or the model-length term given by regularization functional (equation 13).

$$x = W_d(d - Gm) \quad (12)$$

$$x = W_m m \quad (13)$$

For the case of $x_j=0$, objective function (equation 11) need to modified to avoid discontinuity in $\partial\phi/\partial x$ (Farquharson and Oldenburg, 1998). Thus a small user-specified value ϵ is added to equation (11) in order to introduce stability when $x_j=0$. The modified objection function for ℓ_1 measure is then expressed as.

$$\phi(x) = \|(x^2 + \epsilon^2)\|_1^1 \quad (14)$$

Recall equation (10),

$$(G^T W_d^T R_d W_d G + \lambda W_m^T R_m W_m) m = G^T W_d^T R_d W_d d \quad (15)$$

The R functional in equation (15) can be written as

$$R_{ij} = \begin{cases} (x^2 + \epsilon^2)^{-1/2} & i=j \\ 0 & i \neq j \end{cases} \quad (16)$$

Because R is a function of unknown parameter, x , this is a non-linear system, and iterative approach must be used. This is referred to iteratively re-weighted least squares, IRLS, (Wolke and Schwetlick, 1988).

We followed the approach of Farquharson and Oldenburg, (1998), by setting $R = I$ for the first iteration, which result in traditional least squares solution. The estimation of m^i for $i=1$ is used to calculate R in equation (16), and then subsequently substituted again in equation (15) to obtain a new m^{i+1} . The procedure is repeated until the convergence criteria given in equation (17) between successive IRLS iterations are met.

$$\frac{\|m^{k+1} - m^k\|_2}{1 + \|m^{k+1}\|_2} < \tau \quad (17)$$

where τ is a tolerant value.

Two user-defined parameters are now controlling the behavior of the solution of inverse problems: λ , and ϵ . A small value of ϵ is needed to stabilize equation (14), but too small value can introduce instability for any $x_j \rightarrow 0$. On the other hand, a large value of ϵ tend to act more like the traditional regularization parameter, λ when $\epsilon \gg x$ (Minsley, 1997). The damping parameter, λ , can be chosen either by the L-curve method (Hansen, 1994) or by using a user specified small positive value that is $0 < \lambda < 1$.

Since the main objective of the inversion algorithm used in this study is to have minimal intervention by the user, we followed the approach of Farquharson and Oldenburg, (1998) and Zhdanov and Tolstaya, (2004) by plotting $\phi(x)$ for a range of ϵ to determine an optimal balance between these two extremes. This is not computationally expensive because it only requires substituting multiple values of ϵ into equation (14) using the current value of x .

In the following sub sections, building of the L-curve functional and calculating the maximum curvature to obtain the optimal trade-off parameter ϵ are given.

Building the L-curve

The optimal trade-off parameter, ϵ , is calculated based on the L-curve method of Hansen and O’Leary, (1993). The L-curve is a plot, in log-log scale, of corresponding values of the residual and solution norms (Figure 6). In this research, the optimal trade-off value of ϵ is chosen to be within specific range ($10^{-5} \leq \epsilon \leq 1$) divided over 150 points of equal spaces. The L-corner is defined either as maximum curvature (Hansen, 1994) or as the point of tangency with a straight line of negative slope (Reginska, 1996; Oraintara et. al., 2000).

Note that, Hansen, (1994) defined the L-corner as the point of maximum curvature, and the calculation of the inverse problem was repeated for two-hundred different values of regularization parameter to find the L-corner.

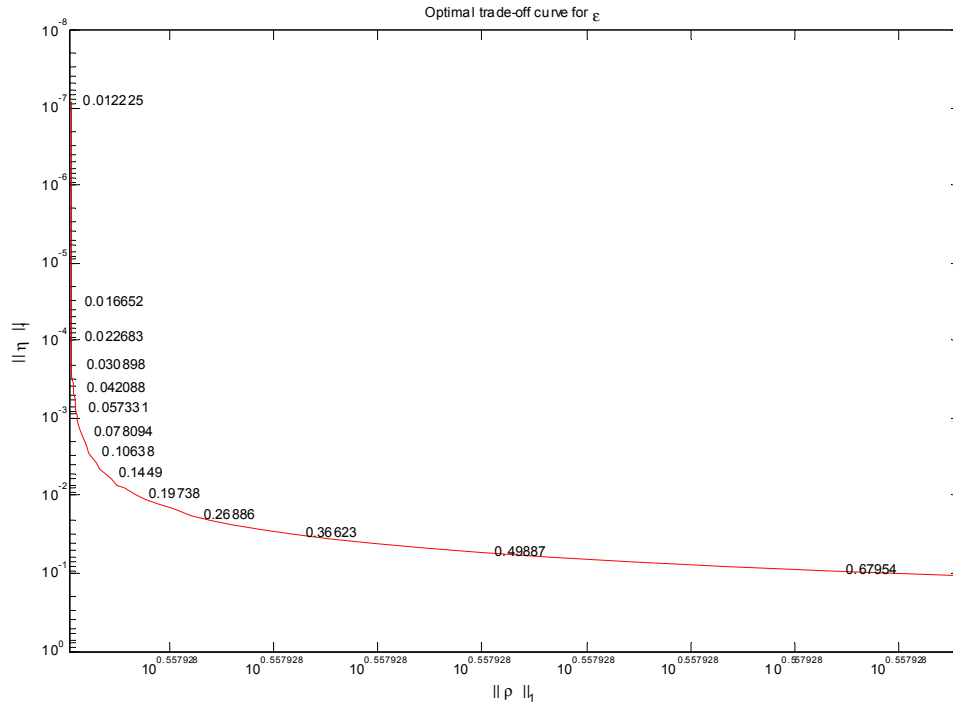


FIG.6. Well 08-08: The L-curve plot of log values of residual and solution norms.

In order to construct the L-curve function given in figure (6), let the x- and y-axes calculated as

$$\rho = \log \left\| (x_d^2 + \epsilon^2) \right\|_1^1 \tag{18}$$

$$\eta = \log \left\| (x_m^2 + \epsilon^2) \right\|_1^1 \tag{19}$$

where x_d and x_m represent the data-misfit and model length terms that were calculated from equations (12 and 13) respectively. The point on the L-curve associated with ϵ is given by $\frac{1}{2}(\rho, \eta)$.

In Figure (6), when ϵ is very large, the curve is essentially a horizontal line in a region called over-regularization region (Oraintara et. al., 2000). Conversely, when ϵ is very small (under-regularization), the curve is basically a vertical line. The transition between these two regions of under and over-regularization corresponds to the “corner” of the L-curve and the associated value of ϵ at this corner is considered as an optimal value of the regularization parameter.

The curvature of L-Curve

The curvature k_ϵ of the L-curve (Calvetti et. al., 2000) is given by

$$k_\epsilon = 2 \frac{\rho''\eta' - \rho'\eta''}{((\rho')^2 + (\eta')^2)^{3/2}} \quad (20)$$

where $'$ and $''$ denotes the first and second differentiation with respect to ϵ . From equations (18 and 19), and $\rho' = -\epsilon\eta'$ (Hansen and O’Leary, 1993), the optimal curvature, \hat{k}_ϵ , is given by

$$\hat{k}_\epsilon = 2 \frac{\eta\rho}{\eta'} \frac{\epsilon^2\eta'\rho + 2\epsilon\eta\rho + \epsilon^4\eta\eta'}{(\epsilon^2\eta^2 + \rho^2)^{3/2}} \quad (21)$$

Note that Hansen, (1994) uses initial k_ϵ obtained in equation (20) with few regularization parameters before and after initial k_ϵ in order to get the optimal maximum curvature \hat{k}_ϵ . The index of the minimum of this maximum curvature is the optimal trade-off parameter $\hat{\epsilon}$. In this study, the associated ϵ to initial k_ϵ curvature estimated in equation (20) is substituted into equation (21) in order to obtain the optimal \hat{k}_ϵ . The index of minimum \hat{k}_ϵ is then cross-referenced with an array of all ϵ_i values used so as to obtain associated optimal trade-off parameter $\hat{\epsilon}$. Figure (7) shows the maximum curvature calculated from L-curve function, while figure (8) shows the optimal $\hat{\epsilon}$ obtained during the IRLS inversion algorithm.

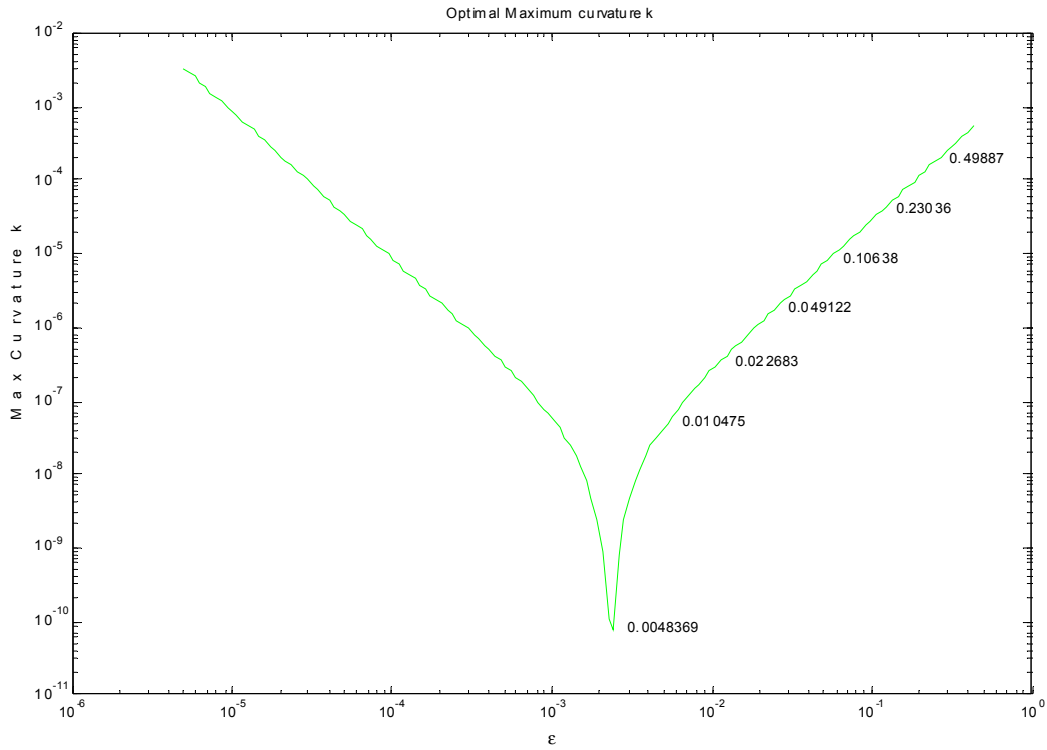


FIG.7. Well 08-08: The optimum maximum curvature \hat{k}_ϵ .

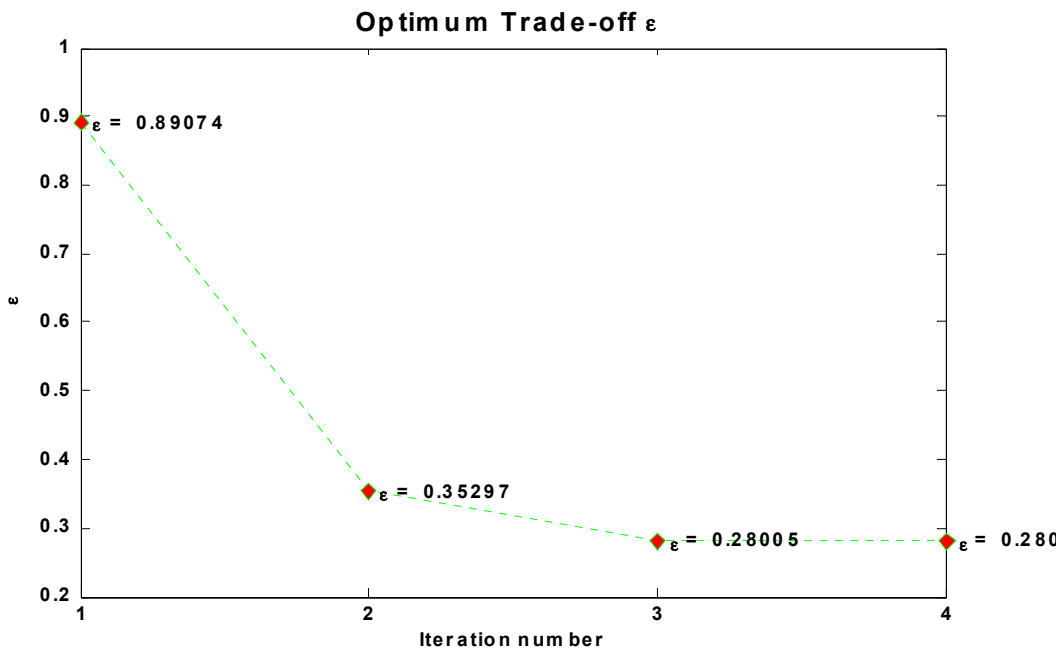


FIG.8. Well 08-08: The optimum trade-off $\hat{\epsilon}$

Model regularization operator W_m

The regularization operator can be either smoothness or compactness. Imposing additional information about the model can constrain the roughness of the inverse operator (Constable et al., 1987) in order to produce a stable model. The purpose of regularization operator in the inverse problem is to introduce stability while recovering models that do not involve complicated features.

Smoothness constraint operator

Common forms of regularization applied to the model are those developed by Tikhonov and Arsenin, (1977) in order to introduce stability through constraints provided by the regularization operator. When the operator is identity matrix ($W_m = \mathbf{I}$, 0th order), a minimum length solution is obtained. If the operator is gradient ($W_m = \nabla$, 1st order), a flat solution is obtained, while a Laplacian operator ($W_m = \nabla^2$, 2nd order) leads to a smooth solution (Ajo-Franklin, et. al., 2007).

Although neither flatness nor smoothness is intrinsic properties of the earth, Tikhonov methods have enjoyed remarkable success, particularly in use of first order finite-difference operator (deGroot-Hedlin, and Constable, 1990). Note that, although these operators introduce stability to inverse algorithm however, some resulting model tends to have very smooth section that may not always realistic (Silva et al., 2001).

Li and Oldenburg, (2000) advocate to select regularization operators that incorporate some constraints that are responsible for observed property variations, such as geological dip or fluid flow in high permeability zone. This also can be the case when a geologic feature such as a dike has material properties that vary over short distances, or where fluid flow occurs along restricted high permeability pathways (Ajo-Franklin et al., 2007).

Compactness constrain operator

Compactness constrain is another stabilizing function that minimizes the area where strong variation in model parameter or discontinuity occur (Portniaguine and Zhdanov, 1999). The compactness constrain operator is non-linear and require the use of model-space in iteratively reweighted least squares (IRLS) sense for effective solution. In the following subsections, three type of compactness constraints are given in some details. The weighted matrix, W_d was set as *identity* matrix during the inversion. Note that due to large numbers of figures generated using different weight methods, I will include only figures that best describe the concept used in this study.

Modified Total-variation method

The total variation approach ($Tv(m) = \|\nabla m\|_{L1}$) was used by Rudin et al. (1992) to reconstruct of noisy and blurred image. This approach was then modified by Acar and Vogel, (1994) so as to introduce stability when model parameters are non differentiable.

The modified total variation method or cumulative sensitivity (Portniaguine and Zhdanov, 1999) is explicitly written as

$$\Lambda_{ij} = (\mathbf{J}^2 + \beta^2)^{1/2} \quad i = 1 : N \quad (22)$$

where \mathbf{J} is the Jacobian matrix, or sensitivity matrix of the data with respect to model parameters $\partial\phi_d / \partial m$ and β is a small fractional number introduced to provide stability.

The Λ_{ij} form a diagonal weighting matrix that allow for solutions away from measurement locations, where sensitivity decreases (Boulangier and Chouteau, 2001; Li and Oldenburg, 1996).

Figure (9) shows measured V_p (green in color), measured density (blue in color) and the predicted section (red in color) in the right side panel. The inverted density log has successfully delineated all lithology layers, and was able to discriminate sandstone reservoir. Figure (10) is associated RMS error during the inversion. From the inverted density log, sand baseline at 2.5 (gm/cm³) can be easily recognized, and deviation from that line depends on the change in lithology at each top.

Minimum support method

Compact body inversion, developed by Last and Kubik (1983) has been used in potential field (Portniaguine and Zhdanov, 1999) as well as in seismic tomography (Ajo-Franklin, 2007) inverse problems, and usually produces a blocky image model (Claerbout and Muir, 1973). Minimum support function, often referred as compactness is based on the minimization of an area (or volume in three-dimensions) metric of the anomaly. Last and Kubik (1983) introduced an area metric, $A(m)$ that is expressed as,

$$A(m) = a_e \lim_{\beta \rightarrow 0} \sum_{i=1}^N \frac{m_i^2}{m_i^2 + \beta} \quad (23)$$

where a_e is the area of a single element, m_i is the i th model parameter, and β is a small number that is introduced to provide stability as $m_i \rightarrow 0$. In the limit of $\beta \rightarrow 0$, the term on the right hand side of equation (23) evaluate to 1 when $m_i \neq 0$, and they become 0 when $m_i = 0$. This metric approximate the area of anomalous region.

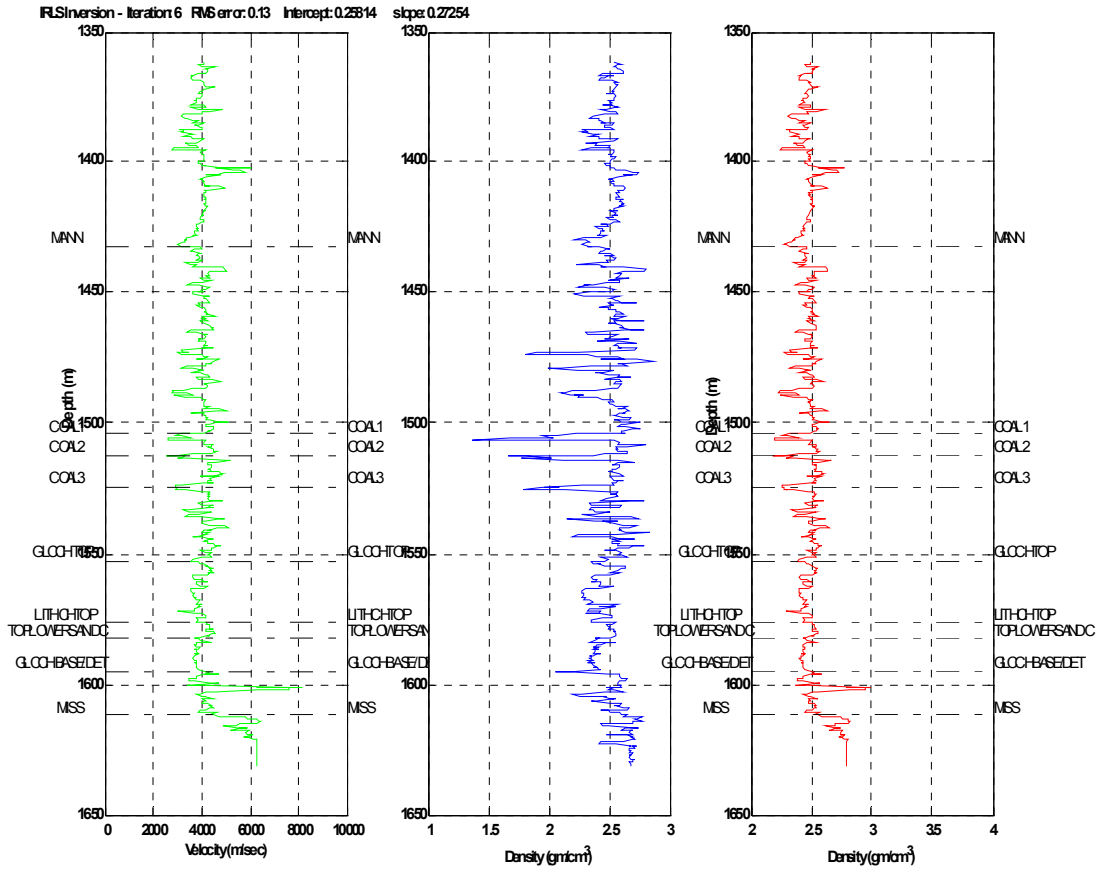


FIG.9. Well 08-08: IRLS inversion of density log using modified total-variation constrain.

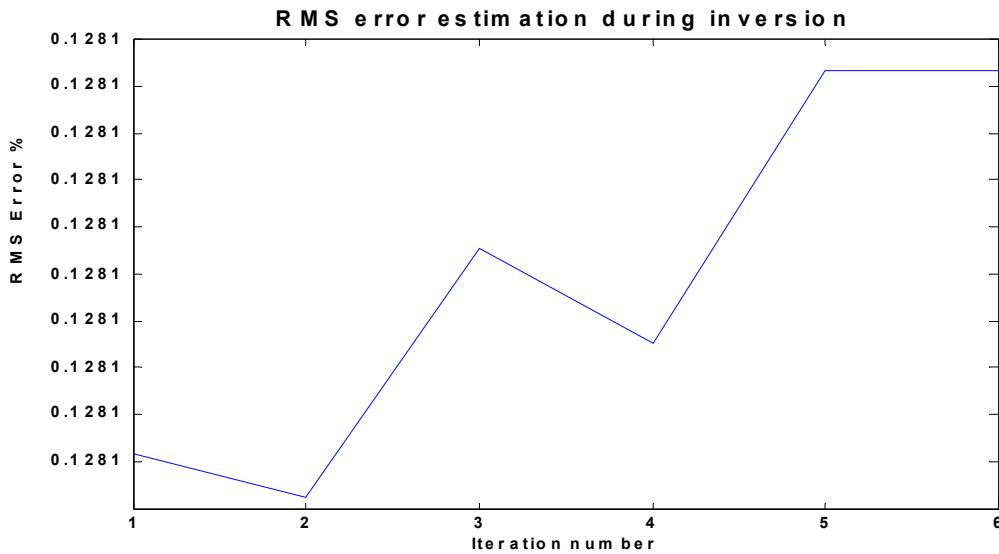


FIG.10. Well 08-08: RMS Error during IRLS inversion using modified total-variation constrain.

A new objective function that incorporate the measure of the area, is given by

$$\phi_d + \lambda^2 \phi_m = \|Gm - d\|_2^2 + \lambda^2 \sum_{i=1}^N \frac{m_i^2}{m_i^2 + \beta} \tag{24}$$

Minimization of objective function yields a least-square problem that is now dependent on model estimate. The new diagonal weighted matrix, W_c that incorporate compactness can be written in explicit form as

$$W_c = (m_{ii}^2 + \beta^2)^{-1/2} \tag{25}$$

The W_c matrix can be viewed as a spatially variable damping matrix with high values in regions where the prior model estimate has a small absolute magnitude (Ajo-Franklin, 2007). The inverted section produced after 6th iteration given in figure (11) shows that compactness constrain is slightly better in resolving very thin layers compared to the cumulative index in figure (9). Figure (12) is a plot of RMS error during the inversion.

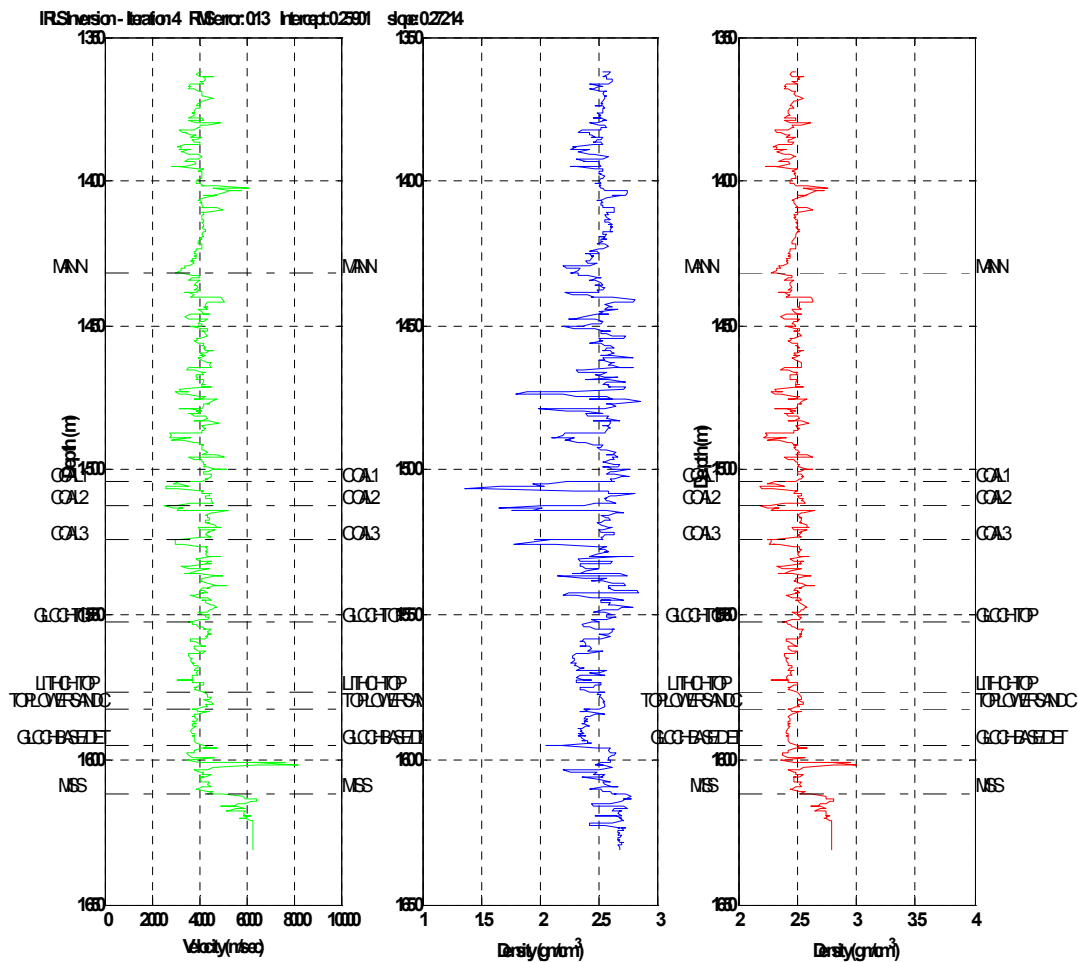


FIG.11. Well 08-08: IRLS inversion of density log using minimum support constrain.

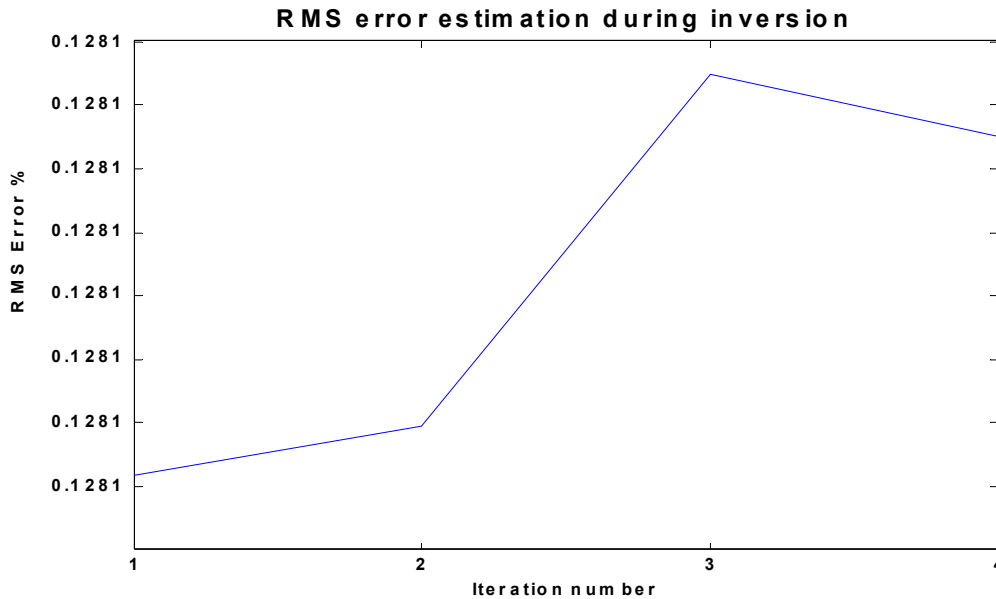


FIG.12. Well 08-08: RMS error during IRLS inversion using minimum support constrain.

Minimum gradient support

A new weighting variable is defined by equation (26), which includes the cumulative constraint (sensitivity weight) scaled by partial derivative of model parameters.

$$\Omega_{ii} = \frac{\nabla m \cdot \nabla m}{\Lambda_{ii}^2} \quad (26)$$

Incorporating of new weight function into traditional least square inverse problem lead to a new objective function that can be expressed as,

$$\phi_d + \lambda^2 \phi_m = \|Gm - d\|_2^2 + \lambda^2 \|\Omega m\|_2^2 \quad (27)$$

Figure (13) shows the inverted section using minimum gradient support constraint, while figure (14) is associated RMS error during the IRLS inversion.

CONCLUSIONS

The proposed inversion density algorithms are effective quantitative approaches. The inverted density log has substantially resolved different subsurface lithology layers, and successfully delineated the sand channel. The re-weighted least square inverse algorithm of density log shows fast convergence towards the final model with few numbers of iterations. The optimum trade-off parameter calculated through inverse algorithm has provided stability to the inverse scheme.

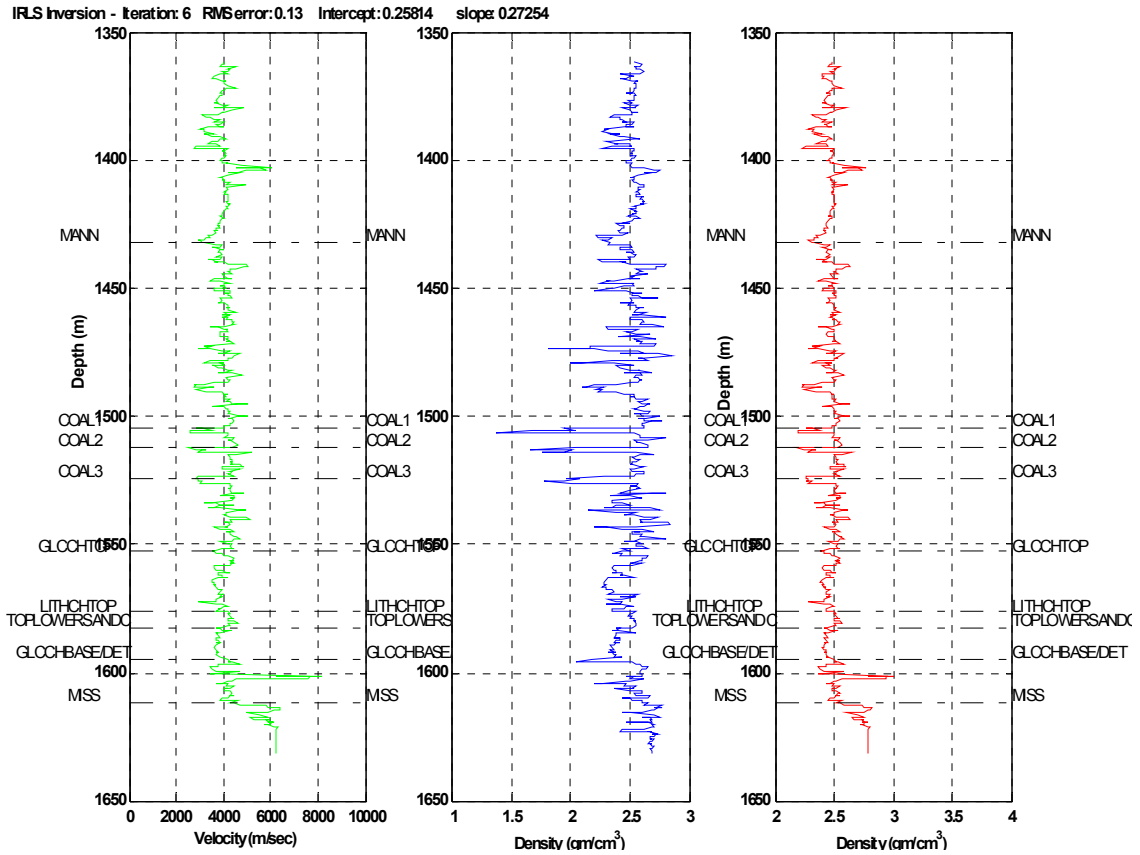


FIG.13. Well 08-08: IRLS inversion of density log using minimum gradient constrain.

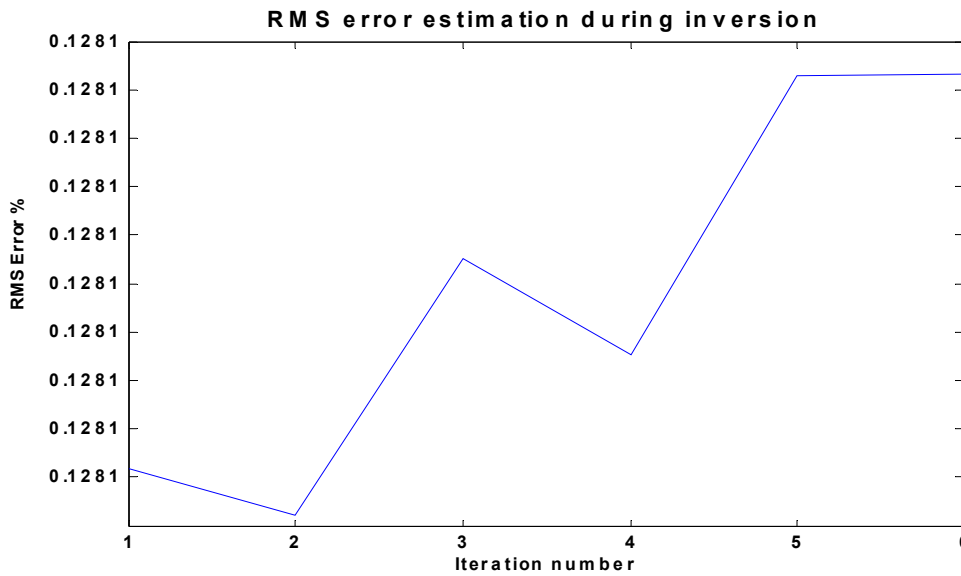


FIG.14. Well 08-08: RMS error during IRLS inversion using minimum gradient constrain

REFERENCES

- Acar, R., and Vogel, C. R., 1994, Analysis of total variation penalty methods: *Inverse Problems*, **10**, 1217–1229.
- Ajo-Franklin, J.B., Minsley B.J. and Daley T.M., 2007, Applying compactness constraints to differential travelttime tomography. *Geophysics*, **72**, 67-75.
- Aster, R.C., Borchers, B. and Thurber, C.H., 2005, *Parameters estimation and inverse problem* : Elsevier Academic Press.
- Boulanger, O., and Chouteau, M., 2001, Constraints in 3D gravity inversion: *Geophys. Prospect.* **49**, 265-280.
- Calvetti, D. Morigi, S., Reichel, L., and Sgallari, F., 2000, Tikhonov regularization and the L-curve for large, discrete ill-posed problems: *J. Comp. Appl. Math.*, **123**, 423-446.
- Chopra, S., and Pruden, D., 2003, Multiattribute seismic analysis on AVO-derived parameters—A case study: *The leading Edge*, **22**, 998-1002.
- Claerbout, J.F. and Muir, F., 1973, Robust modeling with erratic data: *Geophysics*, **38**, 826-844.
- Constable, S.C., Parker, R.L., and Constable, C.G., 1987, Occam's inversion: A practical algorithm for generating smooth models from electromagnetic sounding data: *Geophysics*, **52**, 289-300.
- Dufour, J., Squires, J., Edmunds, A., and Shook, I., 1998, Integrated geological and geophysical interpretation of the Blackfoot area, Southern Alberta: **68th Annual International SEG Meeting, Expanded Abstracts**, 598-601.
- Farquharson, C. G., and Oldenburg, D.W., 1998, Non-linear inversion using general measures of data misfit and model structure: *Geophy. J. Int.*, **134**, 213-227.
- Gardner, G.H.F., Gardner, L.W. and Gregory, A.R., 1974, Formation velocity and density- the diagnostic basis for stratigraphic traps: *Geophysics*, **39**, 770-780.
- Goodway, B. and Tessman, D.J., 2002, Blackfoot 3C/3D test makes the point for VectorSeis : *Special Topic: Land seismic: First Break*, **20**, 116-121.
- Hansen, P. C., 1994, Regularization tools: A MATLAB package for analysis and solution of discrete ill-posed problems: *Numerical Algorithm*, **6**, 1-35.
- Hansen, P. C., and O'Leary, D. P., 1993, The use of L-curve in regularization of discrete ill-posed problems: *SAIM J. Sci. comput.*, **14**, 1487-1503.
- Last, B.J., and Kubik, K., 1983, Compact gravity inversion: *Geophysics*, **48**, 713-721.
- Levenberg, K., 1963. A method of the solution of certain non linear problems in least-squares: *Quarterly of applied mathematics* **2**, 164-168.
- Li, Y., and D.W. Oldenburg, 1996, 3-D inversion of magnetic data: *Geophysics*, **61**, 394-408.
- Li, Y.G., and D.W. Oldenburg, 2000, Incorporating geological dip in formation into geophysical inversions: *Geophysics*, **65**, 148-157.
- Lines, L.R. and Treitel., 1984. Tutorial: A review of least-squares inversion and its application to geophysical problems: *Geophysical Prospecting* **32**, 159-186.

Margrave, G.F., Lawton, D.C., and Stewart, R.R., 1998, Interpreting Channel Sand with 3C-3D Seismic Data: The Leading Edge, **17**, 509-513.

Miller, S.L.M., Aydemir, E.O. and Margrave, G.F., 1995, Preliminary interpretation of P-P, P-S seismic data from Blackfoot broad-band survey: CREWES report, **42**.

Minsley, B.J., 2007, Modeling and inversion of self-potential data: Ph.D. thesis, MIT.

Oraintara, S., Karl, W.C. , Castanon, D.A., and T.Q. Nguyen, 2000, A method for choosing the regularization parameter in linear inverse problems: IEEE- ICIP on Trans. Image Processing.

Pendrel, J., Stewart, R.R., Dufour, J., Goodway, B., and Van Riel, P., 1999, Offset Inversion of the Blackfoot P-wave Data and Discrimination of Sandstone and Shales: Annual Mtg. Canadian Soc. of Expl. Geophys, **52**, 289-300.

Portniaguine, O., and Zhdanov, M. S., 1999, Focusing geophysical inversion images: Geophysics, **67**, 874-887.

Reginska, T., 1996, A regularization parameter in discrete ill-posed problems: *SIAM J. Sci. Comput.*, **17**, 740–749.

Rudin, L. I., Osher, S., and Fatemi, E., 1992, Nonlinear total variation based noise removal algorithms: *Physica D*, **60**, 259–268.

Scales, J.A., Gersztenkorn, A., and Treitel, S., 1988, Fast Lp Solution of Large, Sparse, Linear-Systems - Application to Seismic Travel Time Tomography: *J. Comput. Phys.*, **75**, 314-333.

Silva, J.B.C., Medeiros, W.E., and Barbosa, V.C.F, 2001, Potential-field inversion: Choosing the appropriate technique to solve a geologic problem: *Geophysics*, **66**, 511-520.

Tarantola, A., 1987, *Inverse Problem Theory: Methods for Data Fitting and Model Parameter estimation*: Elsevier Publisher.

Tikhonov, A.N., and Arsenin, V.Y., 1977, *Solutions of ill-posed problems*: Wiley, New York Publisher.

Wahba, G., 1977, Practical approximate solutions to linear operator equations when the data are noisy: *SIAM Journal of numerical analysis*, **14**, 651-667.

Wolke, R., and Schwetlick, H., 1988, Iteratively re-weighted least squares algorithms, convergence analysis, and numerical comparisons: *SIAM Journal of Scientific and statistical computation*, **9**, 907-921.

Wood, J.M., and Hopkins, J.C., 1992, Traps associated with paleo-valleys and interfluves in an unconformity bounded sequence: Lower Cretaceous Glauconitic Member, Southern Alberta, Canada: *The American Association of Petroleum Geologists Bulletin*, **76**, 904-926.

Zhdanov, M., and Tolstaya, E., 2004, Minimum support nonlinear parameterization in the solution of a 3D magnetotelluric inverse problem. *Inverse Problems*, **20**, 937-952.